UWL REPOSITORY

repository.uwl.ac.uk

Advancing energy and indoor environmental quality through integrated co-simulation and multi-objective optimisation for SARS-COV-2 risk mitigation a UK case study

Abbaspour, Atefeh, Bahadori-Jahromi, Ali ORCID logoORCID: https://orcid.org/0000-0003-0405-7146, Janbey, Alan and Tahayori, Hooman (2025) Advancing energy and indoor environmental quality through integrated co-simulation and multi-objective optimisation for SARS-COV-2 risk mitigation a UK case study. Energy Science & Engineering.

This is the Published Version of the final output.

Alternative formats: If you require this document in an alternative format, please contact:
open.research@uwl.ac.uk

ORIGINAL ARTICLE OPEN ACCESS

Advancing Energy and Indoor Environmental Quality Through Integrated Co-Simulation and Multi-Objective Optimisation for SARS-CoV-2 Risk Mitigation: A UK Case Study

Atefeh Abbaspour[1] (ID) | Ali Bahadori-Jahromi[1] | Alan Janbey[2] | Hooman Tahayori[3]

[1]Department of Civil and Environmental Engineering, School of Computing and Engineering, University of West London, London, UK | [2]Research Department, The London College, London, UK | [3]Department of Computer Science and Engineering and IT, Shiraz University, Shiraz, Iran

Correspondence: Atefeh Abbaspour (Atefeh.abbaspour@uwl.ac.uk)

ABSTRACT

In today's modern world, people spend most of their time indoors, making indoor air quality (IAQ) a critical concern, particularly in educational buildings, where densely occupied classrooms demand clean and healthy environments. This study enhances the IAQ of an existing college building in West London by aiming to reduce carbon dioxide (CO_2) concentrations and SARS-CoV-2 infection risk, while maintaining or improving energy efficiency and thermal comfort, assessed using the predicted percentage of dissatisfied (PPD). A multi-objective optimisation was conducted using the Non-dominated Sorting Genetic Algorithm II (NSGA-II). A novel approach combining optimisation with EnergyPlus and CONTAM co-simulation was proposed to obtain the final results. Various scenarios were developed, reflecting different priorities. Energy-saving scenarios increased PPD by 15.3% to 17.9%, while IAQ- and comfort-focused scenarios raised energy consumption by 26.95% to 53.91% but maintained or improved comfort. EC45 as a mixed-priority scenario, along with IAQ-priority scenarios, achieved the lowest average SARS-CoV-2 infection risks (9.6%–10.7%). Meanwhile, other mixed-priority (EP45-ECP33) scenarios reduced PPD by 13.9% and maintained a 17% infection risk with only a 29% increase in energy use. This comprehensive approach demonstrates the potential for achieving healthier indoor environments in educational buildings without excessively compromising energy efficiency or occupant comfort.

1 | Introduction

In the context of designing built environments, energy efficiency and indoor air quality (IAQ) are among the most important factors that should be considered. In particular, IAQ and thermal comfort, which are two key components of the broader concept of indoor environmental quality (IEQ), play a vital role in ensuring occupant satisfaction, health and safety. Maintaining high IEQ standards is essential for creating healthy, comfortable and productive indoor environments. These factors become even more essential for educational buildings (which have a high level of occupant density) as thermal discomfort and low-quality indoor environment can adversely impact the students' learning ability [1] and productivity, as well as staff performance and behaviour [2].

In fact, the lack of indoor fresh air in educational buildings can exacerbate different respiratory [3, 4] and cardiovascular diseases [5], especially in the younger generation, as they spend most of their time at schools and universities. Moreover, the COVID-19 pandemic attracted more attention to the importance of IAQ [6], and it is a fact that the probability of infection in the poorly ventilated places can increase greatly [7, 8].

Furthermore, educational buildings; energy consumption is significant for the nonindustrial sector [9]. According to data provided by the Higher Education Statistics Agency (HESA) [10], higher education (HE) buildings in the UK consumed about 53,000 MWh of energy on average, produced mainly by natural gas and electricity, in the 2020/2021 academic year. This amount of energy consumption has led to nearly 10.8 million $kgCO_2$ emissions. Among the UK universities whose data are available on the HESA, the University of Edinburgh consumed the highest amount of energy and the highest CO_2 emissions during 2020/2021, which were 284,000 MWh and 64.5 million $kgCO_2$, respectively.

Considering these statistics, improving the energy performance of the HE sector can play a major role in reducing the carbon footprint and greenhouse gas emissions [11]. In this case, energy efficiency measures are important to study to find a proper solution for enhancement of the building's energy performance. One of the methods to decrease the energy consumption is adding insulation to the external walls or filling the cavity walls with insulation materials [12, 13].

Ventilation is an effective strategy for enhancing IAQ [14] and can be achieved through natural, mechanical, or hybrid systems (a combination of natural and mechanical ventilation). Consequently, the recommended methods for controlling contaminant spread within a building vary based on the ventilation type present. For example, in naturally or hybrid-ventilated rooms, occupants can enhance IAQ by opening windows to maintain CO_2 levels below 1000 ppm, indicating adequate ventilation. On the other hand, in mechanically ventilated spaces, the supply and return airflows can be exactly set to maintain the required IAQ level without any intervention from the occupants [4].

Several research studies have analysed the role of opening the windows and the ways to set, control and design their opening and airflow using building simulation and Non-dominated Sorting Genetic Algorithm II (NSGA-II) optimisation [15, 16]. In this regard, Nateghi and Kaczmarczyk [17] used jEPlus + EA software, which is also used in multiple studies, for multi-objective NSGA-II optimisation of both opening the window and setting the thermostat temperature in a classroom in two contrasting climates to improve the IAQ, energy consumption, and thermal comfort. The results showed that in more than 50% of the time, all objectives were controlled at the desired level by performing the optimisation.

Optimisation of energy consumption along with thermal and visual comforts (predicted percentage of dissatisfied [PPD] and discomfort glare index [DGI]) was the focus of a study by Naderi et al. [18]. They employed the same software tool to perform an optimisation on an office building, defining variables such as shading control strategy, various slat dimensions and characteristics, and temperature setpoints. Their findings indicated that all three objectives could be simultaneously improved through the careful selection of design variable combinations.

Another study by Chen et al. [19] explored the optimisation of IEQ using EnergyPlus and jEPlus, focusing on a residential building in Hong Kong. Their objectives included daylighting, natural ventilation and thermal comfort, aiming to minimise the duration during which local green building guidelines for qualified IEQ were not met. The optimisation process resulted in an 11.2% reduction in unmet time compared to the baseline case, with a 31.95% improvement in thermal comfort. Furthermore, Aghamolaei and Ghaani [20] addressed the challenge of optimising building retrofitting to improve energy efficiency while preserving indoor thermal comfort, focusing on a residential building. This study introduced a methodology that integrates Parametric Sensitivity Analysis (PSA) with a multi-objective optimisation (MOO) approach, aiming to simplify the process of selecting the most effective retrofit measures.

Baghoolizadeh et al. [13] conducted a similar approach to optimise CO_2 levels, pollutant concentrations and thermal comfort in six residential buildings across various climates. The study used a genetic algorithm to adjust 39 design variables, including heating, ventilation and air conditioning (HVAC) setpoints, clothing insulation levels, and building envelope characteristics. Results showed significant improvements as CO_2 concentration decreased by 17%–30%, pollutant levels by 15%–37%, and thermal comfort by 52%–80%. In another study, Grygierek et al. [15] focused on optimising natural ventilation in classrooms using smart window control systems to improve thermal comfort, IAQ and minimise infection risks. The study performed detailed evaluations of different ventilation strategies, including the impact of smart window systems on indoor environment quality.

Despite these advances, most optimisation studies that include IAQ as one of their objectives rely only on EnergyPlus or other energy performance simulation tools, often without incorporating a dedicated IAQ analysis tool, and typically focus on only CO_2 as the IAQ single indicator, while neglecting other pollutants [12–16]. This study addresses this gap by integrating CONTAM modelling with optimisation through an innovative approach, which enables the inclusion of SARS-CoV-2 transmission risks or unlimited types of indoor contaminants such as particulate matter ($PM_{2.5}$) and Total volatile organic compounds (tVOC) alongside energy performance and thermal comfort optimisation.

In this study, the goal is to optimise energy consumption, IAQ levels and thermal comfort in a college building by considering four variables: indoor temperature, different combinations of hybrid ventilation including various mechanical ventilation rates and window opening, and external wall insulation.

The following sections of the study will detail the research methodology, including the building description, modelling approach, simulation tools, model validation and key conceptual frameworks. The optimisation results will then be presented, followed by an analysis of the findings, evaluation of

performance trade-offs, and a discussion of the final decision-making process. Finally, the conclusions section will summarise the key findings, outline the study's limitations and provide recommendations for future research and practical applications.

2 | Methodology

To achieve the research objective, a novel method is used which combines the optimisation using jEPlus + EA with EnergyPlus and CONTAM co-simulation. The whole process is illustrated in Figure 1.

In this study, EnergyPlus is used to simulate energy consumption and thermal comfort, CONTAM to model multi-zone airflow, contaminant dispersion and infection risk, and jEPlus + EA to conduct NSGA-II multi-objective optimisation. While each tool offers powerful modelling capabilities, they also have limitations. EnergyPlus lacks the ability to simulate detailed interzonal airflow, aerosol transport, or multiple indoor contaminants, which CONTAM addresses effectively. On the other hand, CONTAM does not support thermal comfort or energy performance analysis, which EnergyPlus provides. CONTAM allows for detailed assessment of ventilation strategies and IAQ, including the definition and simulation of an unlimited number of pollutants. Additionally, jEPlus+EA facilitates automated optimisation directly using EnergyPlus outputs and eliminating the need for custom Python scripting or external integration.

This method, therefore, addresses the limitations of using EnergyPlus alone for multi-zone contaminant modelling. Although EnergyPlus includes an "internal network" for ventilation load calculations, it is not capable of modelling the spread of pollutants or viruses within a building's zones [21]. By integrating CONTAM, which enables precise modelling of various contaminants, the methodology fills this gap.

Moreover, unlike most optimisation studies that focus only on CO_2 as an IAQ indicator, this study expands the scope by incorporating viral transmission risks, such as SARS-CoV-2, through the innovative co-simulation and optimisation integration approach. To support decision-making, the simple additive weighting (SAW) method is then applied to the Pareto fronts to select final solutions based on user priorities and different weights assigned to each objective. This comprehensive method offers a more holistic framework, enabling the simultaneous evaluation of IAQ considering an unlimited type of contaminants, energy use, thermal comfort and public health concerns.

2.1 | Building Overview

This study selected a three-story college building located in the Hounslow borough of London, consisting of classrooms, laboratories, offices, etc, chosen as the case study for whole-building modelling (shown in Figure 2). The height of each level, including the plenum, is 3.6 m (plenum excluded height is 2.8 m), and the total floor area is 2500 m^2. The building's ventilation is provided by an air handling unit (AHU) with a different number of supply and return diffusers in each room, where each of the supply diffusers has a rate of approximately 0.011 m^3/s.

The modelled building includes 11 classrooms and six laboratories. This study primarily focuses on improving IAQ in the
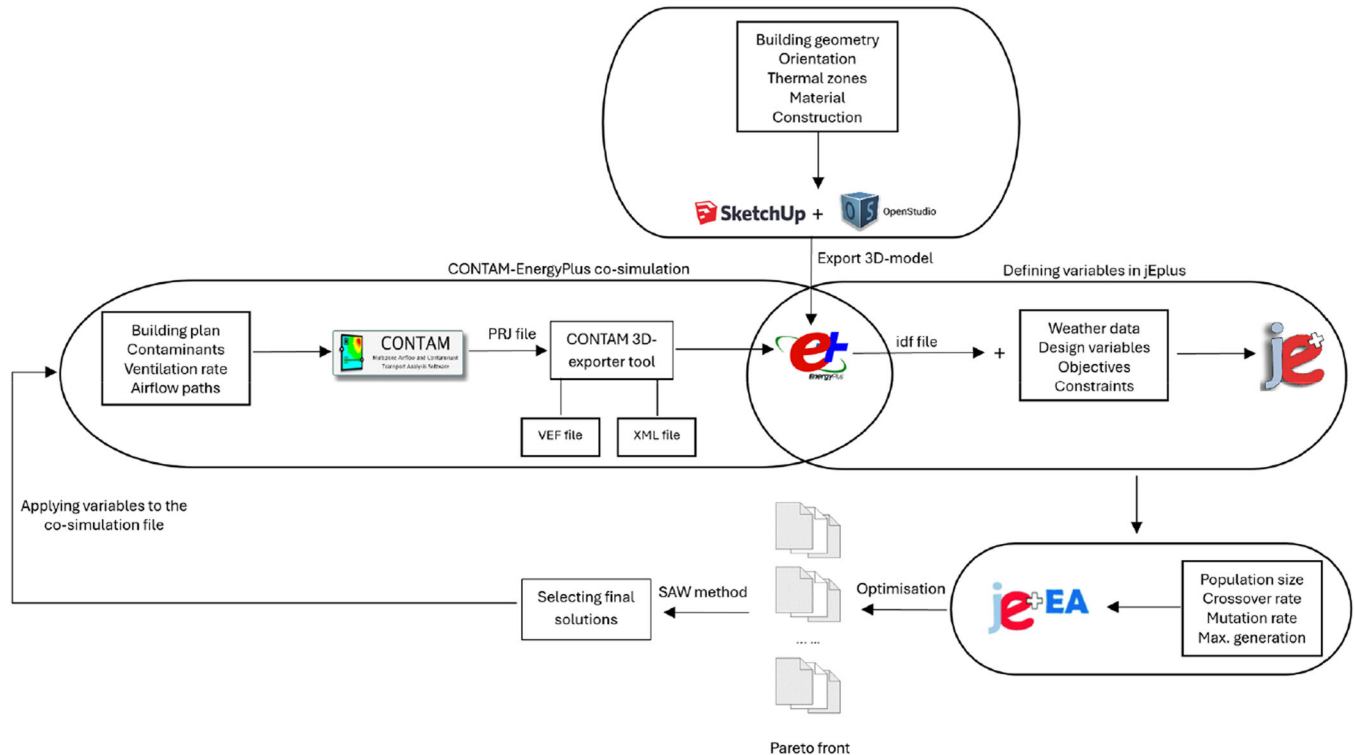

FIGURE 1 | Summary of research methodology.

classrooms and laboratories, where high occupant density and extended occupancy periods are common. However, the entire building is modelled to accurately assess airflow and contaminant spread between zones and floors, as well as to calculate total energy consumption under various scenarios.

All the windows are kept fixed in the building, and the only way of ventilating the rooms is by the AHU. However, the option of windows opening is considered in the optimisation process of the present study. Furthermore, the external walls of the building are cavity walls without any insulation, which leads to higher energy loss. Therefore, adding insulation is considered a method of enhancing the energy performance of the building. Figure 3 shows the supply diffusers installed on the ceiling of rooms and the window shape of the building. The windows' size in all the buildings is 1.35×0.96 m.

To be accurate in determining the IAQ in the building, the real timetable of the college for 2023 was used to define the schedules. Furthermore, the maximum capacity of each classroom for the number of people was considered for modelling and presenting the results (as shown in Table 1). Although not always are the classes fully occupied.

For the weather file, the London Test Reference Year (TRY) weather file from The Chartered Institution of Building Services Engineers (CIBSE) is used in the simulation. Figure 4 shows the

FIGURE 2 | The case study building located in Hounslow, London.

FIGURE 3 | Window and supply diffuser in the building.

weather conditions of the case study, including its temperature and humidity ratio.

2.2 | Building Co-Simulation Process

The building was modelled using two software tools, each addressing different aspects of performance. EnergyPlus was used to simulate energy use and thermal comfort, while CONTAM analysed airflow, contaminant dispersion and IAQ. The CONTAM project file (PRJ) and EnergyPlus IDF were linked via the Contam3DExporter tool, which merges both models into a new IDF for co-simulation.

In this process, the PRJ file is converted into a variable exchange file and XML file, which are packaged into an functional mock-up unit (FMU) along with the CONTAM model. The FMU enables EnergyPlus to co-simulate with other programs, exchanging data such as schedules, airflow rates, output variables, zone temperatures and outdoor conditions. This CONTAM-EnergyPlus co-simulation allows a detailed assessment of how IAQ improvements affect energy performance and thermal comfort, ensuring a comprehensive indoor environment analysis.

2.3 | Defining Contaminants in CONTAM

CONTAM is a useful tool for IAQ analysis as an unlimited number of indoor and outdoor contaminants can be defined in it. By modelling the building in CONTAM, the airflow and dispersion of contaminants between the zones, floors and walls can be simulated. Therefore, in this study, CONTAM was used for an accurate analysis of the IAQ in the optimised cases. Table 2 summarises the key input parameters used for analysing the IAQ in the case study.

CO_2 level is widely recognised as an indicator of IAQ and a measure of the ventilation system's effectiveness in a particular zone. The outdoor CO_2 concentration, as well as its initial level in all zones, is considered to be 400 ppm [24]. Since occupants exhale

TABLE 1 | Characteristics of the most occupied rooms in the building during the summer semester.

Zones		Floor	Volume (m³)	Max. number of occupants	Number of occupied days per week
Classrooms	G11C	GF	304	30	1
	108C	1st	202	20	2
	112C	1st	205	20	5
	115C	1st	181	20	4
	117C	1st	169	20	2
	201C	2nd	231	30	1
	208C	2nd	215	20	2
	212C	2nd	183	20	3
	213C	2nd	137	15	3
	214C	2nd	220	20	1
Laboratories	Computer lab (110CL)	1st	151	15	4
	Electronics lab (210EL)	2nd	153	15	1
	Biology lab (102BL)	1st	78	10	1
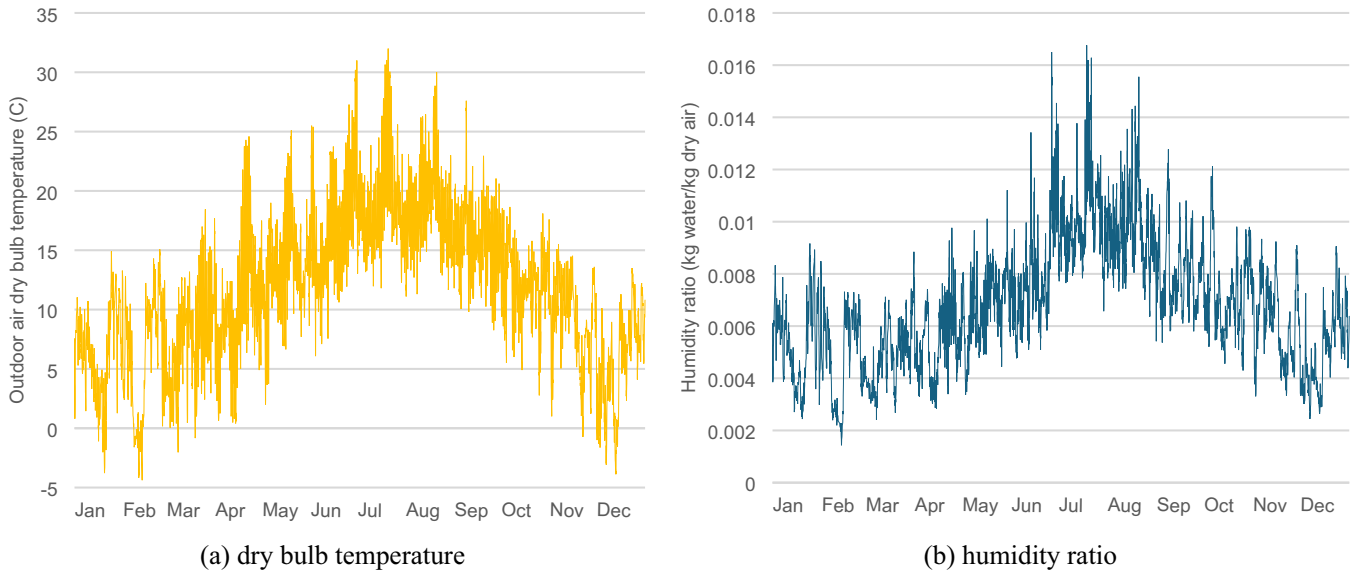
FIGURE 4 | Weather condition of the case study from London TRY weather file: (a) dry bulb temperature and (b) humidity ratio.

CO_2, they are considered the main CO_2 generation source in indoor environments. Various factors, such as activity level, gender and age, influence the CO_2 generation rate. For this study, an average generation rate of 0.0042 L/s, based on typical activity levels across different zones, has been adopted [23].

Furthermore, data from previous research is used to model the SARS-CoV-2 virus in CONTAM. In this regard, a generation rate of 65 quanta/h [21, 25], along with deposition and deactivation rates of 0.24 h^{-1} [27] and 0.63 h^{-1} [28], respectively, are considered. To evaluate the risk of SARS-CoV-2 transmission in indoor spaces, the Wells–Riley equation, as a

widely used model in previous studies, shown in Equations (1) and (2), is employed [21, 29].

$$P_I = N_C/N_S = 1 - \exp(-Iqpt/Q) = 1 - \exp(-n_q) \tag{1}$$

$$n_q = p(1 - M_{inh} \times F_m) \int_{t_1}^{t_2} C(t)dt \tag{2}$$

where P_I is the probability of infection, N_C is the number of infection cases, N_S is the number of susceptibles, I is the

TABLE 2 | Key variables in building IAQ assessment.

Input parameter	Value
Building model	
Type	College building
Types of most occupied rooms	Classroom—Laboratory
Occupancy schedules	Provided based on college's annual time table for 2023
Number of floors	3
Total floor area	2500 m²
Floor height (excluding plenum)	2.8 m
Location and weather file	London—TRY weather file from CIBSE
Ventilation system	Air handling unit
Total ventilation rate	5289 m³/h—calculated and validated in previous study [22]
ACH	0.8–1.0 h⁻¹ [22]
External wall/floor leakage area	2.2 cm²/m² (@4 Pa)
Outdoor air	100%
Recirculating air	0%
CO₂ model	
Source	Respiration
Generation rate	0.0042 L/s [23]
Initial concentration	400 ppm [24]
Deposition rate	0 h⁻¹
Deactivation rate	0 h⁻¹
SARS-CoV-2 model	
Source	Infected person
Generation rate	65 quanta/h [21, 25]
Breathing rate	0.75 m³/h—light activity (whispering and speaking) [26]
Deposition rate	0.24 h⁻¹ [27]
Deactivation rate	0.63 h⁻¹ [28]
Initial concentration	0 quanta

number of infectious sources (infectors), p is the pulmonary ventilation rate of a person (breathing rate) per hour, q is the quanta generation rate per hour, t is the exposure time to the certain microorganism (in hours), Q is the room ventilation rate, and n_q is the number of quanta that have been inhaled. In Equation (2), M_{inh} is the mask inhalation efficiency, F_m is the percentage of mask-wearing and C is the concentration of quanta (quanta/m³). In this study, considering a light activity (whispering and speaking) level for occupants, p is assumed to be 0.75 m³/h [26].

2.4 | Thermal Comfort (TC) Calculation

Thermal comfort reflects occupants' satisfaction with their surrounding environment [30, 31] and is crucial in building design due to its impact on well-being and productivity. The widely used Fanger model, developed in 1970 [32], evaluates thermal comfort based on six parameters, including air temperature, mean radiant temperature (MRT), relative humidity, air velocity, clothing insulation and metabolic rate [33]. It calculates the predicted mean vote (PMV) and the predicted percentage of dissatisfied (PPD), which estimates the proportion of occupants likely to feel uncomfortable. PMV ranges from cold (−3) to hot (+3), with 0 being neutral. A PMV between −0.5 and +0.5 corresponds to a PPD below 10%, meaning fewer than 10% of occupants are dissatisfied [31, 33]. Equation (3) demonstrates the relationship between PMV and PPD.

$$PPD = 100 - 95 \times \exp^{(-0.03353 \times PMV^4 - 0.2179 \times PMV^2)} \qquad (3)$$

This equation shows that as the PMV deviates further from zero, the PPD increases, indicating a higher percentage of occupants are likely to feel uncomfortable. EnergyPlus allows users to input the necessary parameters to calculate PMV and PPD based on the Fanger model. In the present study, PPD is calculated in EnergyPlus using the following inputs and assumptions derived from ASHRAE handbook of fundamentals and ASHRAE 55 [31, 34]: (1) metabolic rates for different zones range from 1.0, 1.1 and 1.2 met for classrooms, offices and laboratories, respectively, (2) air velocity is considered 0.1 m/s, (3) clothing level ranges from 1 clo for the coldest months where typical winter indoor clothing is considered to 0.5 clo for the warmest months as the typical summer indoor clothing, (4) air relative humidity and temperature are derived from EnergyPlus results and (5) MRT is calculated using "zone averaged" method of EnergyPlus.

2.5 | Model Validation

2.5.1 | IAQ Model

To validate the accuracy of the CONTAM simulation results, CO_2 concentrations were monitored using two types of IAQ data loggers. Three Netatmo data loggers and three Temtop M2000 2nd data loggers were installed in various locations: classrooms 112C and 214C, the electronic lab 210EL, an office on the ground floor, and the canteen near the kitchen.

The Temtop M2000 2nd is equipped with a nondispersive infrared (NDIR) sensor for CO_2 measurement, offering a range of 0–5000 ppm, with an accuracy of ±50 ppm ±5%. Calibration was performed according to the manufacturer's instructions, which involved placing the device in a well-ventilated outdoor area for several minutes and then initiating the zero-calibration process through the device's menu interface to establish a baseline CO_2 concentration. The Netatmo monitors also use NDIR sensors with a measurement range of 0–5000 ppm and are equipped with automatic calibration, which was enabled during the monitoring period.

The CONTAM model of the building was developed, incorporating factors such as room volumes, occupancy profiles, ventilation rates and other parameters influencing IAQ. This allowed the simulation to run under similar conditions to those present during the data collection period. The validation process involved comparing the simulated CO_2 concentrations from the CONTAM model with the measured values obtained from the IAQ sensors. Two key statistical metrics were employed to evaluate the accuracy of the simulation: the mean relative error (MRE) and the correlation coefficient (r).

2.5.2 | Thermal Performance Model

To model the building's energy consumption and thermal comfort in EnergyPlus, a 3D model was created in SketchUp and exported to OpenStudio to define materials and construction. The geometry was built by accurately specifying properties of walls, windows, floors and the roof. Figure 5 shows the SketchUp schematic of the college.

The simulation model was validated by comparing EnergyPlus-predicted energy use with actual consumption data to ensure realistic performance and to compare the tools used. This comparison helped in calibrating the model, making necessary adjustments to input parameters such as occupancy patterns, equipment efficiency and weather conditions to align the simulation closer to actual performance. The Actual energy data, including gas and electricity bills from 2017 to 2022, was provided by building management, and the average usage over these years was used for comparison.

2.6 | NSGA-II Multi-Objective Optimisation (MOO)

In this study, the NSGA-II multi-objective optimisation (MOO) algorithm was used to optimise three conflicting objectives: annual energy consumption (t1), CO_2 concentration as an IAQ indicator (t2) and PPD as a thermal comfort indicator (t3). Since improving one objective often worsens another, NSGA-II effectively identifies optimal trade-offs, known as Pareto fronts, which represent non-dominated solutions where no single solution excels in all objectives [35].
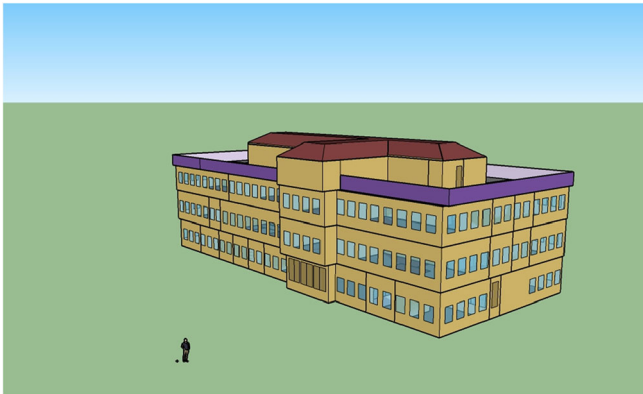

FIGURE 5 | Sketchup model of the building.

The optimisation was performed using jEPlus and jEPlus+EA software developed by Yi Zhang [36]. Evolutionary Algorithms (EAs) start with a random population of solutions, iteratively evaluate and select better ones, and generate new variants until sufficient solutions are found or a time limit is reached [36]. Figure 6 shows the EA optimisation flowchart.

In this regard, the design variables and objectives were defined in the jEPlus, and then optimisation control parameters, including population size, crossover rate, mutation rate and maximum generation, were determined in the jEPlus + EA, which were set to 20, 100%, 20% and 200, respectively. Additionally, three constraints for each objective were defined to ensure that the resulting Pareto fronts represent solutions that are not only optimised but also feasible in real-world scenarios. These constraints, detailed in Table 3, were important in shaping the Pareto fronts to reflect more practical and appli-

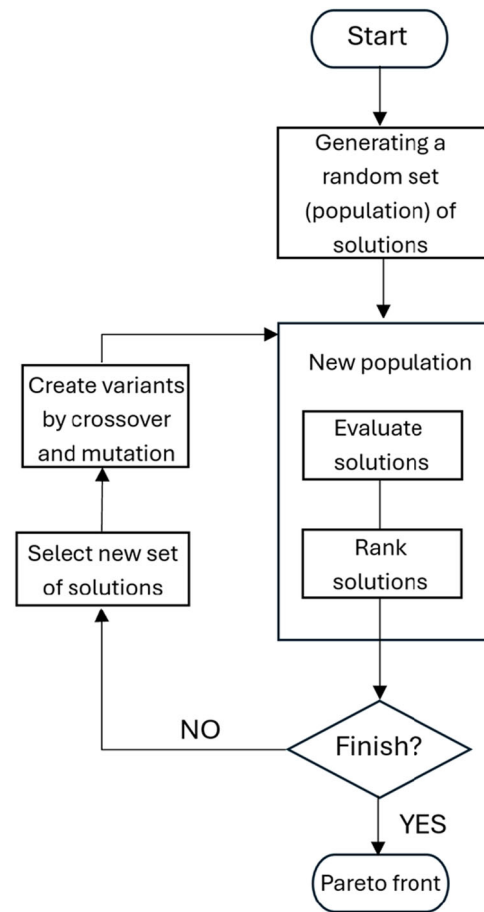**FIGURE 6** | Flowchart of optimisation process using EA [36].

TABLE 3 | Constraints set for the optimisation.

Objectives	Constraint
Energy consumption	< 500,000 kWh
CO_2 concentration	< 1000 ppm
PPD	< 50%

cable outcomes. The optimisation was then carried out in jE-Plus + EA and the Pareto front was created.

2.6.1 | Design Variables

Four parameters were considered as variables in the optimisation: heating setpoint, fraction of window opening, external wall insulation thickness and ventilation rate. Table 4 presents the list of variables and their respective ranges. The heating setpoint was varied from 20°C to 24°C, with the baseline set at 21°C. According to the guidelines for energy efficiency in educational buildings published by the UK government [37], the 21°C is suitable setpoint for rooms where occupants are inactive or sick and overall 20°C is typically ideal for a school.

The fraction of window opening ranged from fully closed (0) to fully open (1) in 10% intervals. EPS insulation (Expanded Polystyrene) was added to the external walls, with thickness varying from 0.01 to 0.15 m in 0.02 m intervals.

Finally, the ventilation rate is set based on the number of people in the room, rather than being a constant amount as it currently is in the building. The rate can be adjusted from a minimum of 0.005 m³/s.p (per person), based on ASHRAE recommendations [38], to a maximum of 0.02 m³/s.p, in intervals of 0.001 m³/s.p. It should be noted that the CIBSE recommendation is 0.01 m³/s.p [39], and the Building Bulletin 101 guidelines recommend 0.008 m³/s.p [40], both of which fall within this range. Furthermore, cases with the building's actual ventilation rate are also considered in the optimisation to determine whether changing the ventilation rate is necessary when other variables change, assuming the ventilation rate is at its baseline level.

2.6.2 | Method of Selecting the Final Cases

The optimisation will result in several Pareto fronts, each acceptable in different cases depending on the priorities of the objectives. In other words, selecting the most favourable point in the optimisation results depends on the preferences of the decision maker. Therefore, the SAW method, a well-known multi-criteria decision-making (MCDM) approach, was used to find the final optimum solution. In optimisation studies, SAW has proven to be one of the most effective methods in selecting representative Pareto-optimal solutions [41, 42].

The SAW method involves three key steps [43]. First, the decision matrix (three objective amounts from Pareto fronts) is normalised to a common scale (0 to 1) using Equation (4). This

equation is applied when the objectives should be minimised, assigning higher normalised values to lower amounts (the minimum amount will have a value of 1, and the maximum amount will be 0).

$$f_{\mathrm{norm},i}(x) = \frac{\max(f_i(x)) - f_i(x)}{\max(f_i(x)) - \min(f_i(x))} \tag{4}$$

where $f_{\mathrm{norm},i}(x)$ is the normalised value of each objective, $\max(f_i(x))$ and $\min(f_i(x))$ are the maximum and minimum values among all the Pareto fronts, and $f_i(x)$ is each objective's value in each case of Pareto fronts.

Second, various weights were assigned to the three objectives of the study, with the sum of the weights equal to 1. These weights reflect the relative importance of each objective and are multiplied by the normalised values to obtain weighted normalised values. In each case, one of the objectives has more or equal importance than the other two to include different preferences in the real world. Third, the weighted values for each alternative were aggregated to calculate a final score, ranking the alternatives based on these scores to determine the best option. Equation (5) illustrates the second and third steps of the SAW method.

$$\begin{aligned} \text{SAW score} = W_{\mathrm{E}} \times f_{\mathrm{norm,E}}(x) + W_{\mathrm{IAQ}} \times f_{\mathrm{norm,IAQ}}(x) \\ + W_{\mathrm{PPD}} \times f_{\mathrm{norm,PPD}}(x) \end{aligned} \tag{5}$$

where W_{E}, W_{IAQ} and W_{PPD} are the assigned weights for each objective, including energy consumption, CO_2 concentration and PPD, respectively. Figure 7 illustrates the assigned values of W in the SAW method.

The scenarios are divided into 13 cases based on different weight distributions for energy consumption, CO_2 concentration and PPD. In scenarios E70, E60, and E50, energy consumption has the highest priority (70%, 60% and 50%, respectively). Similarly, C70, C60, and C50 prioritise CO_2 concentration, while P70, P60 and P50 prioritise PPD with the same respective weights. Scenarios EC45, EP45 and CP45 assign 45% weight to two objectives and 10% to the third, while ECP33 assigns equal weight (around 33%) to all three.

Cases with the highest SAW scores were applied to the EnergyPlus-CONTAM co-simulated model to compare CO_2 concentration and SARS-CoV-2 infection risk (as the selected contaminant) using CONTAM, while EnergyPlus provided energy consumption and PPD values. Since airflow data (infiltration,

TABLE 4 | Design variables defined for the optimisation.

Parameters	Variables	Range	Impacting objective	Interval	Unit
P0	Windows opening area fraction	0–100	IAQ–TC energy use	10	%
P1	Heating setpoint	20–24	TC energy use	1	°C
P2	Air flow rate per person	0.005–0.02	IAQ–TC energy use	0.001	m³/s
P3	External wall insulation thickness	0 and 0.01–0.15	TC energy use	0.02	m

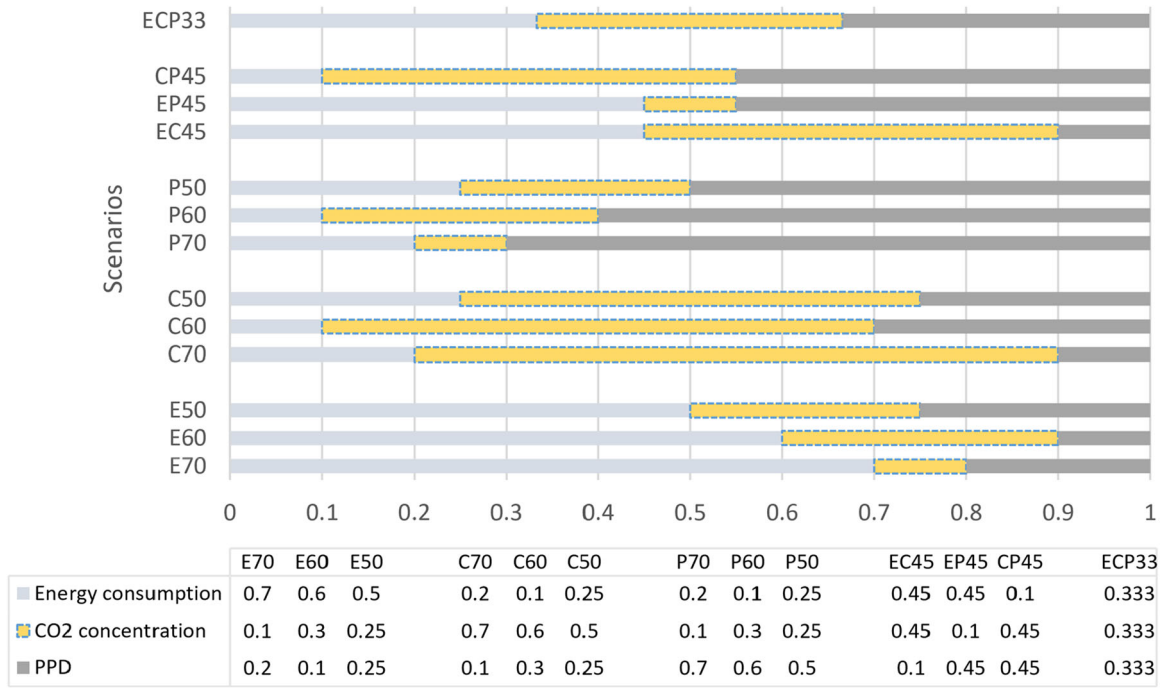|	E70	E60	E50	C70	C60	C50	P70	P60	P50	EC45	EP45	CP45	ECP33
Energy consumption	0.7	0.6	0.5	0.2	0.1	0.25	0.2	0.1	0.25	0.45	0.45	0.1	0.333
CO2 concentration	0.1	0.3	0.25	0.7	0.6	0.5	0.1	0.3	0.25	0.45	0.1	0.45	0.333
PPD	0.2	0.1	0.25	0.1	0.3	0.25	0.7	0.6	0.5	0.1	0.45	0.45	0.333

FIGURE 7 | Assigned weights for the objectives in the SAW method.

TABLE 5 | Mean relative error (MRE) and correlation coefficient (r) in three validation periods.

Zones	Room type	Summer semester 15 May–22 May		Spring semester 23 November–30 November		Autumn semester 20 February–27 February	
		r	MRE	r	MRE	r	MRE
112C	Classroom	0.87	0.14	0.85	0.14	0.84	0.18
210EL	Laboratory	0.74	0.10	0.81	0.13	0.80	0.10
214C	Classroom	0.95	0.04	0.74	0.07	0.88	0.04
Office room	Office	0.67	0.20	0.65	0.19	0.79	0.12

exfiltration and mixing) came from CONTAM, the results were more accurate than using EnergyPlus alone.

3 | Results

3.1 | Validation Results

To perform the IAQ model's validation, data from the IAQ sensors and simulation outputs were synchronised over three periods for each room, which allowed for a point-by-point comparison. Any incomplete or erroneous sensor data, such as periods where sensors failed to log values correctly, were excluded from the analysis to ensure that only valid data points were used in the validation process. Table 5 presents a comparison between simulated and measured CO_2 levels across different zones, classified by room types and over three different time periods.

Furthermore, Figure 8 illustrates a comparison of the data from data loggers and simulation results for three zones in various time periods. Based on Evans' classification [44, 45], the correlation coefficient (r) is classified into different ranges to describe the strength of the relationship between two sets of data. The classifications are as follows: very weak (0.00–0.19), weak (0.20–0.39), moderate (0.40–0.59), strong (0.60–0.79) and very strong (0.80–1.00).

Data in Table 5 shows that for classrooms like 112C and 214C, the correlation coefficients are consistently very high across all time periods, falling between 0.84 and 0.95. According to Evans' classification, this indicates a very strong correlation between the simulated and measured CO_2 concentrations. Moreover, in the laboratory (210EL) and office room, the correlation is strong in most cases, with r values ranging from 0.65 to 0.79. These values are considered acceptable when compared to findings from other research and guidelines [46, 47].

In addition, to validate the thermal performance model, Figure 9 presents a monthly comparison of energy consumption as calculated by EnergyPlus simulation against the actual data.

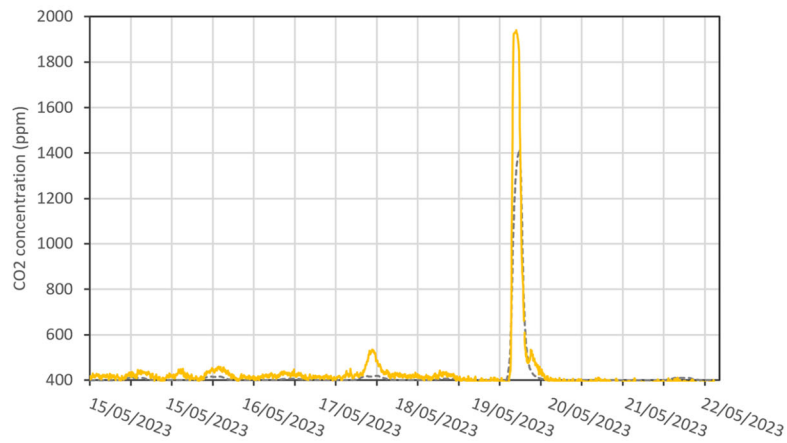The annual energy consumption of EnergyPlus model is 321,418.7 kWh, leading to a 7.02% error from the actual annual consumption of 345,697.48 kWh. These low error percentages indicate that, while monthly trends may vary, the simulated
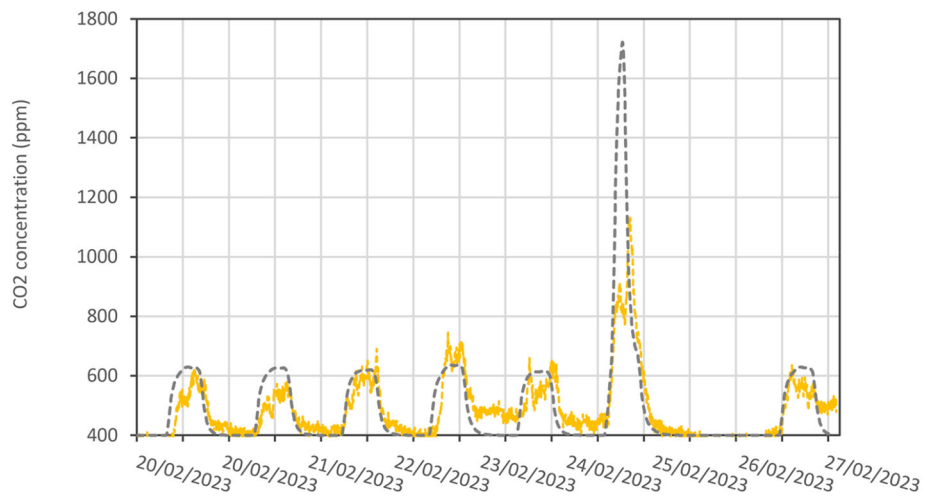
210EL- February
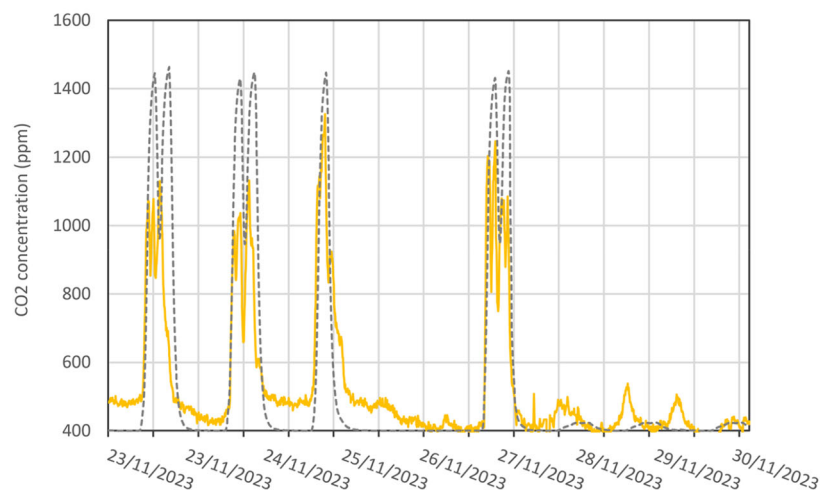
112C- November

214C-May

------ Measured   ------ Simulation

FIGURE 8 | Comparison of CO_2 concentration from measured data and simulation results.
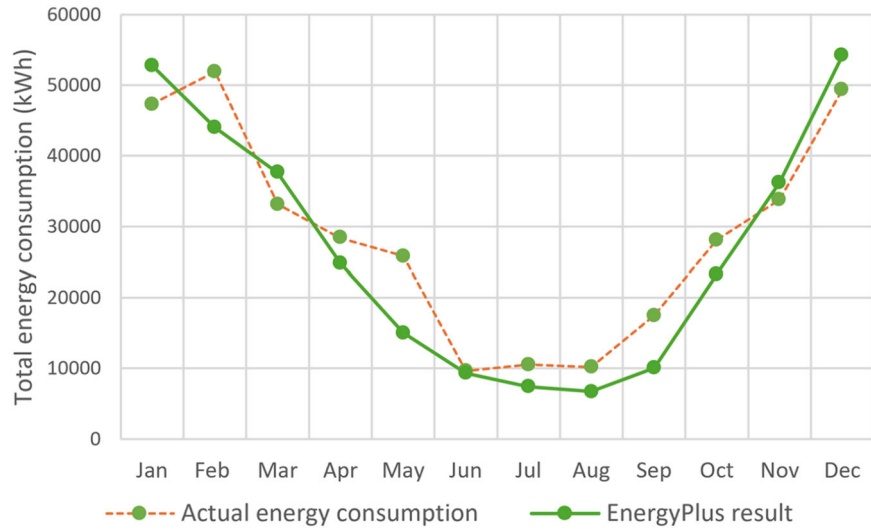
FIGURE 9 | Comparison of simulation results with actual energy consumption.
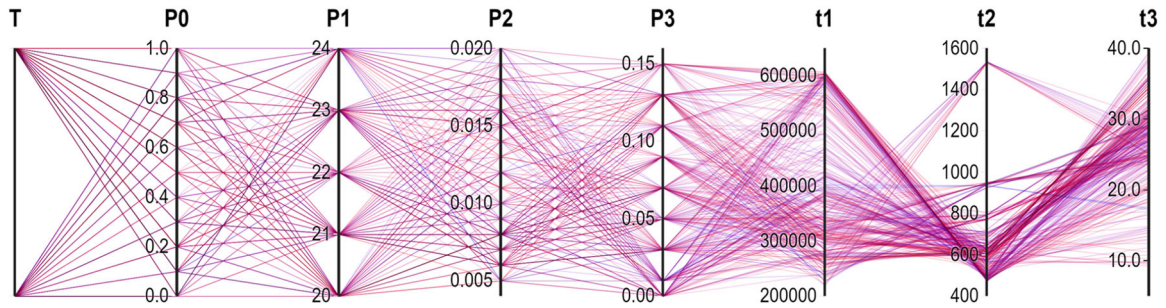

FIGURE 10 | Parallel-coordinates plot of all explored solutions.

model provides a reasonable approximation of the building's total annual energy demand.

3.2 | Optimisation Results

The optimisation process ran for 21 iterations, exploring 413 solutions, of which 210 were Pareto fronts. Figure 10 shows the parallel-coordinates plot of the explored solutions. The first column in this figure (T) represents the two initial files: one using the actual (baseline) ventilation rates, and the other using demand-controlled ventilation based on the number of occupants. P0, P1, P2 and P3 are the design variables explained in Table 4, and t1, t2 and t3 are the objectives discussed in Section 2.6.

Among all the solutions, the highest utilised amount for P0 was 0.2, which was used in 60 solutions. For P1, temperatures of 21°C and 23°C were used 104 and 97 times, respectively. For P2, 0.008 m³/s.p was used 74 times. For P3, the highest used insulation thickness was 0.03 m, used 56 times, followed by 0.07 and 0.13 m, each used 52 times.

The Pareto fronts from the optimisation are shown in Figure 11 as green dots. The three objectives are paired in each plot to better understand their interactions. In this figure, most PPD values, including the maximum and minimum values, fall between 450 and 700 ppm CO_2 levels. Moreover, amounts of the

design variables resulting from the SAW analysis of various preference cases (Figure 7) and the building's baseline condition are presented in Table 6.

3.3 | Final Values of Objectives Using Co-Simulation

3.3.1 | Energy Consumption and PPD

The final results were obtained by applying the values of the design variables in the defined scenarios to the CONTAM-EnergyPlus co-simulation files. The results of the co-simulation are presented in Table 7. This table shows a significant reduction in energy consumption (11.23%–18.94% decrease) in the energy priority scenarios. However, this reduction results in increase of PPD (15.3%–17.9% increase), indicating a decline in occupant comfort.

3.3.2 | CO_2 Levels and SARS-CoV-2 Probability of Infection

As the building has many zones, four rooms with the highest peak CO_2 concentrations were selected to present the results of contaminant levels. These include three classrooms: 117C, 212C and 213C, and the computer lab: 110CL. Characteristics of these zones are summarised in Table 8. Since these rooms are located
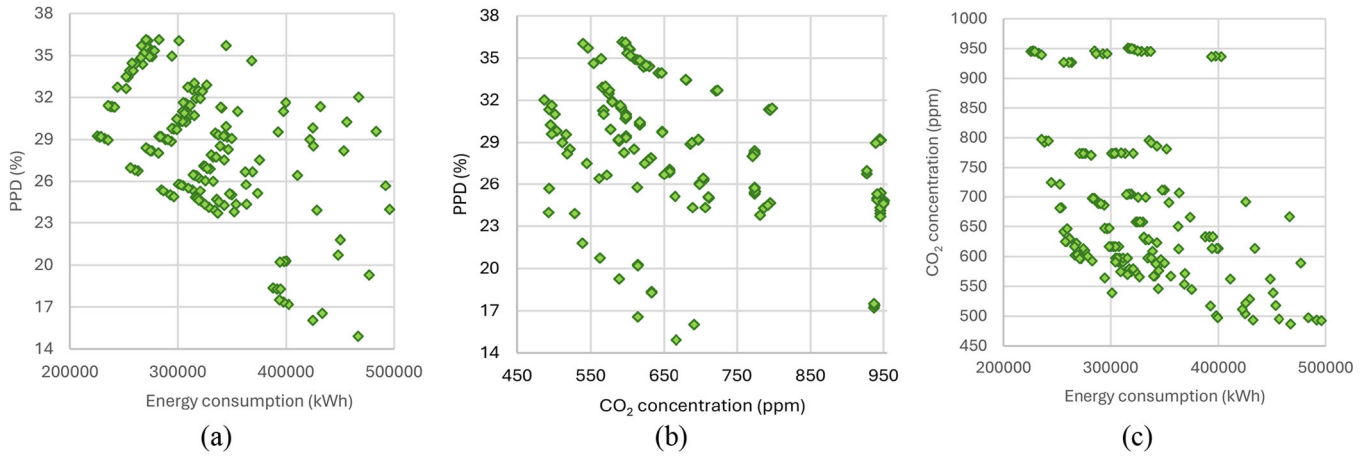
FIGURE 11 | Pareto front of the optimisation with three objectives.

TABLE 6 | Design variables of selected cases with different priorities.

Priority	Baseline/ optimised scenarios	Fraction of window opening (0-1)	Heating setpoint (°C)	Air flow rate Baseline	Air flow rate Per person (m³/s)	Insulation thickness (m)
—	Baseline	0.0	21	✓	—	0.0
Energy	E70	0.1	20	✓	—	0.15
	E60	0.6	20	✓	—	0.15
	E50	0.5	20	✓	—	0.11
				✓		
IAQ	C70	0.9	21	—	0.006	0.03
	C60	0.4	22	—	0.007	0.11
	C50	0.5	22	—	0.006	0.01
Thermal comfort	P70	0.1	23	—	0.007	0.05
	P60	0.1	23	—	0.007	0.05
	P50	0.2	23	—	0.006	0.11
Energy and IAQ	EC45	0.7	20	—	0.005	0.13
Energy and PPD	EP45	0.2	23	—	0.005	0.11
IAQ and PPD	CP45	0.2	23	—	0.006	0.11
All	ECP33	0.2	23	—	0.005	0.11

on different sides and floors of the building, the natural ventilation resulting from wind and stack effect will vary for each room. The average and maximum CO_2 concentrations of these zones under various scenarios are presented in Table 9.

According to Table 9, 212C shows the highest CO_2 level among all zones in baseline case. Consequently, it shows a significant reduction in CO_2 levels, particularly in IAQ-priority scenarios (up to 52.3% in the average level reduction in C70). Maximum levels reductions in 212C also highlight significant improvements (up to 62.2% in C70) which is the highest value among all

four rooms. 117C shows a similar trend to 212C with the highest average reduction of up to 52.9% in IAQ-priority cases.

In addition to CO_2 levels, the SARS-CoV-2 probability of infection (P_I) on the peak day of virus levels in a year was calculated for the selected scenarios. A comparison of each scenario's performance in reducing the P_I is presented in Figure 12.

Each peak in Figure 12 represents a class session during the day. The P_I is calculated only for the occupied hours of the

zones. The spikes indicate that as occupants are more exposed to an infector, the risk of infection increases. The goal is to decrease the maximum P_I in each session.

4 | Discussion

The co-simulation results show that IAQ-priority scenarios increase energy use by 26.95% to 44.7% but significantly reduce CO_2 levels. However, their impact on thermal comfort (PPD) is mixed, with slight improvements (up to 15.5%) or small increases (up to 1.2%) compared to the baseline. The thermal comfort priority scenarios result in a 42.77% to 53.91% increase in energy consumption from the baseline to achieve a lower PPD, ranging from an 18.6% to 22.3% decrease from the baseline. In these scenarios, the average infection probability (P_I) in all rooms is around 16%. Slightly higher P_I values (12.6%–21%) are observed in PPD-energy mixed priority scenarios (EP45 and

ECP33). However, Scenarios prioritising IAQ (C70, C50) and EC45 achieve the lowest average P_I between 9.6% to 10.7% across all classrooms.

These trade-offs between IAQ and comfort improvement and higher energy use are consistent with other multi-objective optimisation studies [17, 20] that balanced these factors against energy in buildings, which also reported that achieving better comfort or air quality typically results in increased energy use. However, unlike the present study, those studies did not model contaminant transport or infection risk.

Among energy-priority scenarios, E70 with only 10% window opening leads to significant CO_2 reductions of 27.4%–31%. Increasing window opening to 50% in E60 further lowers average CO_2 by 17% in a 117C classroom and maximum levels by 35% in 212C classroom. However, even in these energy-priority cases, CO_2 peaks occasionally exceed 1000 ppm (the limit indicating adequate minimum ventilation in classrooms [40]), which shows that ventilation is still inadequate at some times. On the other hand, IAQ priority scenarios in which the window is open from at least 40% to 90%, and ventilation rates range from 0.006 to 0.007 m³/s.p, achieve the lowest CO_2 concentrations.

Results of comparing mixed priority scenarios indicate that while ventilation through window opening helps with reducing average CO_2, mechanical ventilation is more effective at controlling short-term peaks, especially when window use is inconsistent, as supported by previous findings [22, 48]. This focus on IAQ indicators beyond energy and thermal comfort aligns partially with [13], who also used a genetic algorithm to simultaneously improve CO_2-based IAQ and thermal comfort; however, their work remained within EnergyPlus and did not simulate a detailed multi-zone analysis of contaminant transport by co-simulating EnergyPlus with CONTAM or similar tools.

The cumulative percentage plots in Figure 13 provide insight into which scenarios contribute most to the overall performance of each objective. For the IAQ analysis, the maximum levels of CO_2 and P_I in 1 year for the 212C classroom are presented. As shown in Figure 13, the baseline scenario occupies a mid-range position in cumulative percentage distributions for energy consumption and PPD, indicating that performance for these objectives can either improve or worsen relative to the baseline depending on the scenario. However, for IAQ (Figure 13c,d), all scenarios lead to an enhancement compared to the baseline, as the baseline scenario consistently ranks last. Scenario EC45

TABLE 7 | Annual energy consumption and average PPD of different scenarios.

Priority	scenarios	Annual energy consumption (kWh)	Average PPD (%) all occupied zones
—	Baseline	321,418.7	19.17
Energy	E70	260,553.0	22.1
	E60	285,341.9	22.6
	E50	284,286.6	22.6
IAQ	C70	407,925.4	19.4
	C60	464,917.7	16.2
	C50	443,097.2	16.8
Thermal comfort	P70	494,425.8	14.9
	P60	494,425.8	14.9
	P50	458,700.5	15.6
Energy and IAQ	EC45	319,660.0	22.5
Energy and PPD	EP45	414,105.3	16.5
IAQ and PPD	CP45	458,700.5	15.6
All	ECP33	414,105.3	16.5

TABLE 8 | Characteristics of four selected zones to present IAQ results.

Zones	Floor	Area (m²)	Baseline mechanical ventilation rate (m³/h)	Max. number of occupants	External wall orientation
117C	1st	60	164	20	Southwest
212C	2nd	65	123	20	Northeast
213C	2nd	49	164	15	Southwest
110CL	1st	54	123	15	Northeast

TABLE 9 | Average and maximum annual CO_2 concentration in different scenarios.

		CO₂ level							
		212C		**117C**		**110CL**		**213C**	
Priority	**Scenarios**	**Ave.**	**Max.**	**Ave.**	**Max.**	**Ave.**	**Max.**	**Ave.**	**Max.**
—	Baseline	1244.2	2079.6	1239.9	1901.2	1019.0	1569.0	1106.5	1607.2
Energy	E70	865.7	1763.6	855.3	1550.2	740.2	1323.2	787.3	1339.4
	E60	672.7	1034.5	645.4	1003.7	610.1	885.5	618.7	932.5
	E50	688.7	1104.0	659.1	1064.3	621.3	928.6	630.3	971.8
IAQ	C70	593.5	785.6	583.9	787.4	565.5	721.2	570.2	748.7
	C60	617.7	818.0	610.1	837.7	591.3	768.5	596.2	802.7
	C50	620.7	845.0	610.4	861.0	590.8	768.9	595.9	816.3
Thermal comfort	P70	687.6	920.7	690.2	937.7	644.6	880.8	670.4	911.6
	P60	687.6	920.7	690.2	937.7	644.6	880.8	670.4	911.6
	P50	663.5	929.2	662.0	953.4	626.5	883.4	643.6	911.3
Energy and IAQ	EC45	618.6	847.7	607.1	856.4	584.8	781.5	591.2	813.7
Energy and PPD	EP45	684.9	998.8	681.9	1029.6	639.8	938.5	661.4	975.2
IAQ and PPD	CP45	663.5	929.2	662.0	953.4	626.5	883.4	643.6	911.3
All	ECP33	684.9	998.8	681.9	1029.6	639.8	938.5	661.4	975.2

appears as an efficient solution, as in Figure 13a,c,d, it is among the lowest contributors to contaminant levels and energy usage.

As shown in Figure 14, the normalised comparison of each scenario highlights the trade-offs among energy consumption, thermal comfort and IAQ across various scenarios and each scenario's performance compared to the baseline condition. In this regard, scenarios EP45 and ECP33 suggest a moderate trade-off between all the objectives. These scenarios lead to a 28.88% increase in annual energy consumption, which is a moderate increase compared to other scenarios that can lead to more than a 42% increase. PPD in these scenarios decreases by 13.9% compared to the baseline. Moreover, maximum and average CO_2 levels in all classes are below 1000 ppm, with an average decrease of CO_2 levels from the baseline in all rooms by 42%. Furthermore, the average transmission risk of the virus in all sessions is about 17%.

However, if energy consumption should not be increased under any circumstances and contaminants' level should be at lower levels, then the best choice would be EC45. This scenario achieves almost the same energy use to the baseline case (0.55% increase from baseline) and comes with a 17.4% increase on average PPD. However, it results in a 47% decrease in CO_2 levels (never exceeding 1000 ppm over a year) and a 10.7% average P_I in all rooms.

In the selected scenarios, the ventilation rate is $0.005 \, m^3/s.p$, which aligns with the ANSI/ASHRAE 62.1 regulation for educational facilities [38]. They also suggest adding external wall insulation ranging from 0.11 to 0.13 m. The key differences in scenarios' results stem from variations in the thermostat setpoints and window opening fractions (20°C and 0.7 for EC45 vs. 23°C and 0.2 for EP45 and ECP33). According to the results, increasing the heating setpoint by 3°C significantly impacts

energy consumption, regardless of the 71% reduction in window opening in scenarios EP45 and ECP33. In another study, an increase in the heating setpoint was also identified as a cause of a sharp rise in total energy consumption [13]. This highlights that the heating setpoint plays a more dominant role in increasing energy consumption than window opening, as its effect is constant across all zones, while reduced window openings are limited to occupied periods and have a much smaller influence on overall energy savings.

In this study, the integrated methodology demonstrates significant advantages in analysing the trade-offs between energy use, IAQ and thermal comfort. Compared to using EnergyPlus or CONTAM alone, the co-simulation offers a more comprehensive approach by capturing both energy dynamics and pollutant dispersion. Furthermore, although this study employed a detailed simulation framework and real building data, several limitations remain. For instance, the use of fixed ventilation rates and occupancy schedules does not capture the variability of real-world building operations. CONTAM assumes well-mixed conditions within each zone and overlooks spatial gradients and directional airflow. Additionally, the Wells–Riley model used for infection risk estimation simplifies complex factors such as breathing rates and interpersonal distance. These limitations should be considered when interpreting the findings, particularly for real-world applications.

5 | Conclusion

This study introduces a novel methodology that integrates EnergyPlus and CONTAM co-simulation with NSGA-II multi-objective optimisation to explore trade-offs between energy efficiency, IAQ and thermal comfort in a UK educational building.
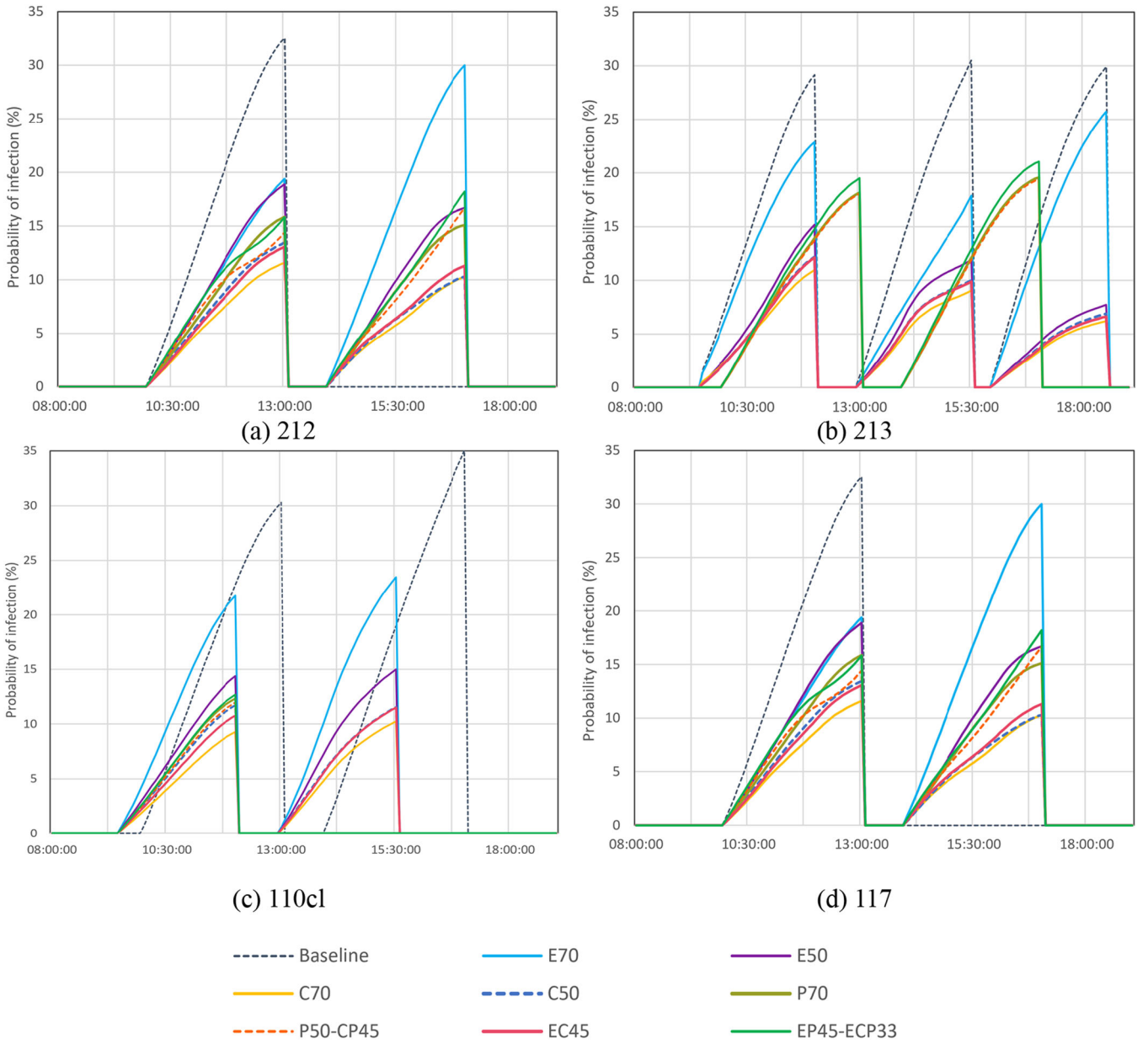
FIGURE 12 | Probability of infection (P_I) in four zones under different scenarios on peak day of virus levels in a year. (a) 212, (b) 213, (c) 110CL and (d) 117.

The findings suggest that improving IAQ and thermal comfort can be achieved without excessively compromising energy efficiency by adopting mixed-priority strategies. For instance, EC45, as a mixed-priority scenario, stands with the scenarios prioritising IAQ (C70, C50) as having the lowest SARS-CoV-2 infection probabilities, averaging between 9.6% and 10.7% across all classrooms. These results emphasise the importance of good IAQ and balanced optimisation strategies in minimising the risk of SARS-CoV-2 infection.

Additionally, the study emphasises the importance of flexible and adaptive building management systems that can respond to varying conditions and priorities. The results also indicate that while natural ventilation improves average IAQ, it can sometimes fail as maximum CO_2 levels exceed the limit. On the other hand, consistent airflow from mechanical ventilation may result

in higher average CO_2 levels, but leads to lower maximum CO_2 levels under the same conditions.

Furthermore, the study highlights that the heating setpoint plays a more dominant role in increasing energy consumption than window opening, as its effect is constant across all zones, while reduced window openings is limited to occupied periods and have a much smaller influence on overall energy savings.

Despite the study's limitations, such as the well-mixed assumption in CONTAM, the simplified virus spread model, and fixed parameters in EnergyPlus (e.g., occupancy schedules), the framework represents a step forward compared to traditional single-tool approaches that often overlook IAQ or infection risk considerations. Future studies are encouraged to incorporate real-time occupancy sensing and adaptive
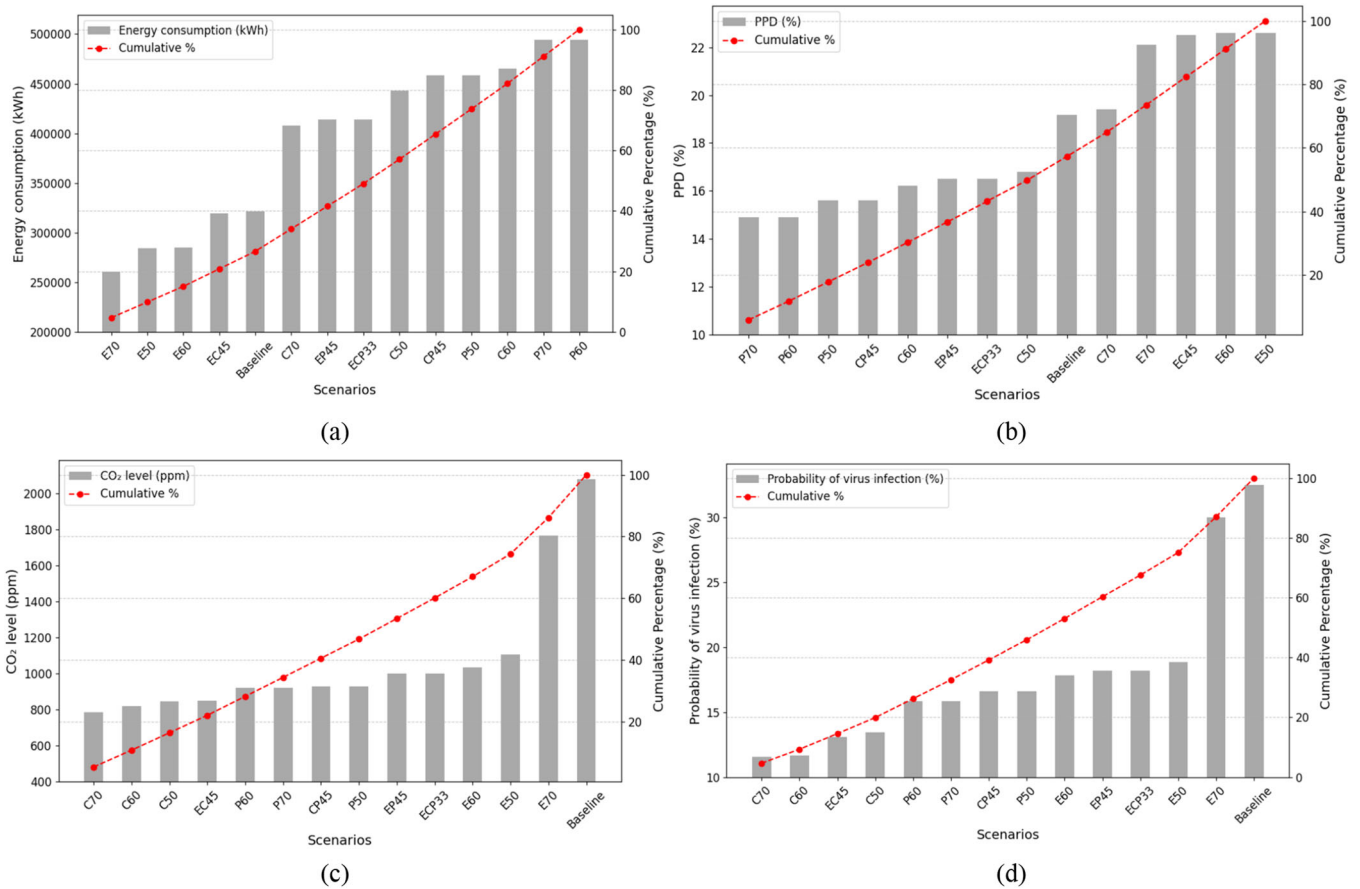
FIGURE 13 | Cumulative percentages distribution of (a) energy consumption, (b) thermal comfort (PPD), (c) IAQ (maximum CO_2 levels) and (d) IAQ (maximum P_I) in 212C classroom across scenarios.
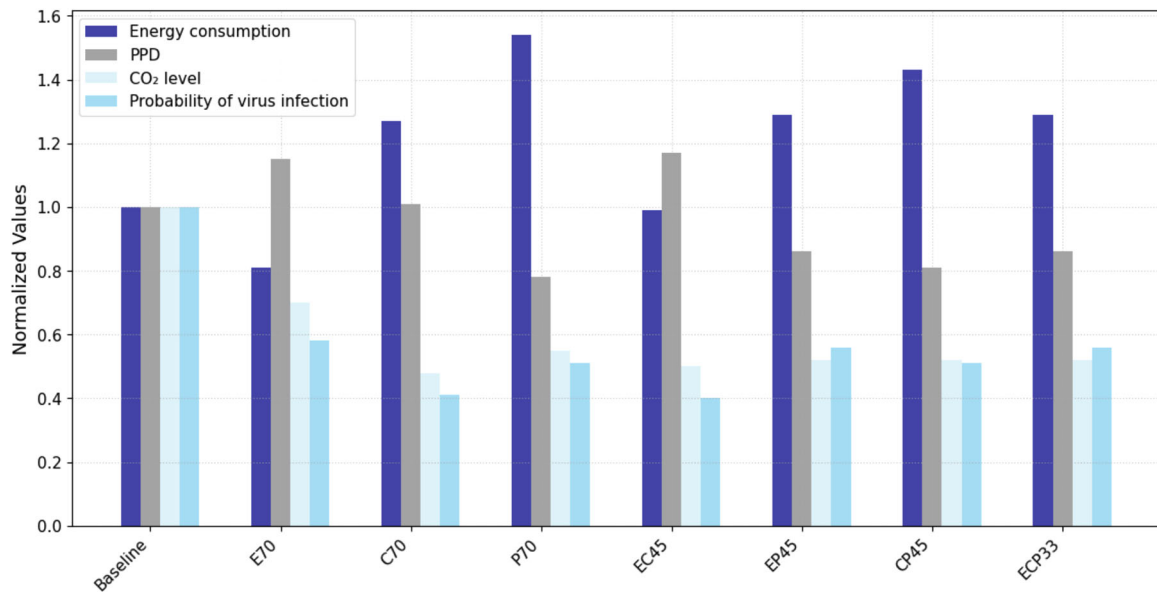

FIGURE 14 | Trade-offs between energy consumption, PPD, along with the maximum CO_2 level and probability of virus infection in the one-year period in classroom 212C.

ventilation control strategies to more accurately capture dynamic building usage, particularly in educational settings. Advanced optimisation methods, such as reinforcement learning or hybrid metaheuristics, could also be explored to enhance the simultaneous management of energy use, IAQ and thermal comfort under varying indoor and outdoor conditions. Further research can also evaluate the life cycle costs and environmental impacts of IAQ improvement strategies to support more

sustainable and economically viable decisions. Finally, the integrated simulation and optimisation approach can be applied to a wider range of building types and climate zones to uncover building-specific optimisation pathways.

Finally, this study provides stakeholders with actionable guidance for optimising IEQ in high-occupancy spaces by offering practical insights into the implications of prioritising one objective over others. Furthermore, the findings of this study can be applied to other educational buildings with similar weather conditions. The study also emphasises the need for regular monitoring and adjustment of indoor environmental parameters to ensure optimal conditions.

Author Contributions

Atefeh Abbaspour: conceptualisation, formal analysis, investigation, methodology, software, validation, visualisation, writing – original draft, writing – review and editing. **Ali Bahadori-Jahromi:** conceptualisation, methodology, project administration, supervision, validation, writing – review and editing. **Alan Janbey:** project administration, resources, supervision, writing – review and editing. **Hooman Tahayori:** supervision, validation, writing – review and editing.

Conflicts of Interest

The authors declare no conflicts of interest.

Data Availability Statement

Data that support the findings of this study are available from the corresponding author upon reasonable request.

References

1. P. Barrett, F. Davies, Y. Zhang, and L. Barrett, "The Impact of Classroom Design on Pupils' Learning: Final Results of a Holistic, Multi-Level Analysis," *Building and Environment* 89 (2015): 118–133.

2. S. Barbhuiya and S. Barbhuiya, "Thermal Comfort and Energy Consumption in a UK Educational Building," *Building and Environment* 68 (2013): 1–11.

3. M. Simoni, I. Annesi-Maesano, T. Sigsgaard, et al., "School Air Quality Related to Dry Cough, Rhinitis and Nasal Patency in Children," *European Respiratory Journal* 35 (2010): 742–749.

4. S. Mentese, N. A. Mirici, T. Elbir, et al., "A Long-Term Multi-Parametric Monitoring Study: Indoor Air Quality (IAQ) and the Sources of the Pollutants, Prevalence of Sick Building Syndrome (SBS) Symptoms, and Respiratory Health Indicators," *Atmospheric Pollution Research* 11, no. 12 (2020): 2270–2281.

5. R. D. Brook, S. Rajagopalan, C. A. Pope, et al., ""Particulate Matter Air Pollution and Cardiovascular Disease: An Update to the Scientific Statement From the American Heart Association," *Circulation* 121, no. 21 (2010): 2331–2378.

6. A. J. Aguilar, M. L. de la Hoz-Torres, N. Costa, P. Arezes, M. D. Martínez-Aires, and D. P. Ruiz, "Assessment of Ventilation Rates Inside Educational Buildings in Southwestern Europe: Analysis of Implemented Strategic Measures," *Journal of Building Engineering* 51 (2022): 104204, https://doi.org/10.1016/j.jobe.2022.104204.

7. A. Zivelonghi and M. Lai, "Mitigating Aerosol Infection Risk in School Buildings: The Role of Natural Ventilation, Volume, Occupancy and CO_2 Monitoring," *Building and Environment* 204 (2021): 108139, https://doi.org/10.1016/j.buildenv.2021.108139.

8. F. Ascione, R. F. De Masi, M. Mastellone, and G. P. Vanoli, "The Design of Safe Classrooms of Educational Buildings for Facing Contagions and Transmission of Diseases: A Novel Approach Combining Audits, Calibrated Energy Models, Building Performance (BPS) and Computational Fluid Dynamic (CFD) Simulations," *Energy and Buildings* 230 (2021): 110533, https://doi.org/10.1016/j.enbuild.2020.110533.

9. IEA, "IEA ECBC Annex 36," 2004.

10. HESA, Energy by HE Provider and Academic Year (2022), https://www.hesa.ac.uk/data-and-analysis/estates/table-2.

11. A. Evandro, et al., "The Carbon Footprint of Buildings: A Review of Methodologies and Applications," *Renewable and Sustainable Energy* 94, no. December 2017 (2018): 1142–1152, https://doi.org/10.1016/j.rser.2018.07.012.

12. H. Seraj, A. Abbaspour, and A. Bahadori-Jahromi, "Towards a Hybrid Retrofit Planning Framework: A Data-Driven Tool for Energy Retrofit in Residential Buildings," *Energy and Built Environment*, no. May (2025), https://doi.org/10.1016/j.enbenv.2025.05.013.

13. M. Baghoolizadeh, M. Rostamzadeh-Renani, M. Hakimazari, and R. Rostamzadeh-Renani, "Improving CO_2 Concentration, CO_2 Pollutant and Occupants' Thermal Comfort in a Residential Building Using Genetic Algorithm Optimization," *Energy and Buildings* 291, no. April (2023): 113109, https://doi.org/10.1016/j.enbuild.2023.113109.

14. N. A. Megahed and E. M. Ghoneim, "Indoor Air Quality: Rethinking Rules of Building Design Strategies in Post-Pandemic Architecture," *Environmental Research* 193 (2021): 110471, https://doi.org/10.1016/j.envres.2020.110471.

15. K. Grygierek, S. Nateghi, J. Ferdyn-Grygierek, and J. Kaczmarczyk, "Controlling and Limiting Infection Risk, Thermal Discomfort, and Low Indoor Air Quality in a Classroom Through Natural Ventilation Controlled by Smart Windows," *Energies* 16, no. 2 (2023): 592.

16. G. M. Stavrakakis, P. L. Zervas, H. Sarimveis, and N. C. Markatos, "Optimization of Window-Openings Design for Thermal Comfort In Naturally Ventilated Buildings," *Applied Mathematical Modelling* 36, no. 1 (2012): 193–211.

17. S. Nateghi and J. Kaczmarczyk, "Multi-Objective Optimization of Window Opening and Thermostat Control for Enhanced Indoor Environment Quality and Energy Efficiency in Contrasting Climates," *Journal of Building Engineering* 78 (2023): 107617, https://doi.org/10.1016/j.jobe.2023.107617.

18. E. Naderi, B. Sajadi, M. A. Behabadi, and E. Naderi, "Multi-Objective Simulation-Based Optimization of Controlled Blind Specifications to Reduce Energy Consumption, and Thermal and Visual Discomfort: Case Studies in Iran," *Building and Environment* 169 (2020): 106570, https://doi.org/10.1016/j.buildenv.2019.106570.

19. X. Chen, H. Yang, and K. Sun, "A Holistic Passive Design Approach to Optimize Indoor Environmental Quality of a Typical Residential Building in Hong Kong," *Energy* 113 (2016): 267–281, https://doi.org/10.1016/j.energy.2016.07.058.

20. R. Aghamolaei and M. R. Ghaani, "Balancing the Impacts of Energy Efficiency Strategies on Comfort Quality of Interior Places: Application of Optimization Algorithms in Domestic Housing," *Journal of Building Engineering* 29, no. August 2019 (2020): 101174, https://doi.org/10.1016/j.jobe.2020.101174.

21. S. Yan, L. L. Wang, M. J. Birnkrant, J. Zhai, and S. L. Miller, "Evaluating SARS-CoV-2 Airborne Quanta Transmission and Exposure Risk in a Mechanically Ventilated Multizone Office Building," *Building Environment* 219, no. February (2022): 109184, https://doi.org/10.1016/j.buildenv.2022.109184.

22. A. Abbaspour, A. Bahadori-jahromi, A. Janbey, P. B. Godfrey, and S. Amirkhani, "Enhancing Indoor Air Quality and Regulatory Compliance: An In-Depth Comparative Study on Ventilation Strategies and Their Impact on SARS-CoV-2 Transmission Risk," *Sustainability* 16, no.1 (2024): 271, https://doi.org/10.3390/su16010271.

23. A. Persily and L. de Jonge, "Carbon Dioxide Generation Rates for Building Occupants," *Indoor Air* 27, no. 5 (2017): 868–879, https://doi.org/10.1111/ina.12383.Carbon.

24. S. Harrington, M. Mulville, and S. Stravoravdis, "The Relationship Between Ventilation Rates in Schools and the Indoor Airborne Transmission Potential of COVID-19," *Architectural Engineering and Design Management* (2023): 1–18, https://doi.org/10.1080/17452007.2023.2263519.

25. G. Buonanno, L. Stabile, and L. Morawska, "Estimation of Airborne Viral Emission: Quanta Emission Rate of SARS-CoV-2 for Infection Risk Assessment," *Environment International* 141 (2020): 105794, https://doi.org/10.1016/j.envint.2020.105794.

26. M. Z. Bazant and J. W. M. Bush, "A Guideline to Limit Indoor Airborne Transmission of COVID-19," *Proceedings of the National Academy of Sciences* 118, no. 17 (2021): e2018995118, https://doi.org/10.1073/pnas.2018995118.

27. T. Moreno, R. M. Pinto, A. Bosch, et al., "Tracing Surface and Airborne SARS-CoV-2 RNA Inside Public Buses and Subway Trains," *Environment International* 147 (2021): 106326, https://doi.org/10.1016/j.envint.2020.106326.

28. N. van Doremalen, T. Bushmaker, D. H. Morris, et al., "Aerosol and Surface Stability of SARS-CoV-2 as Compared With SARS-CoV-1," *New England Journal of Medicine* 382 (2020): 1564–1567.

29. W. S. Dols, B. J. Polidoro, D. Poppendieck, and S. J. Emmerich, *NIST Technical Note 2095, A Tool to Model the Fate and Transport of Indoor Microbiological Aerosols* (FaTIMA, 2020).

30. ISO 7730:2005, *Ergonomics of the Thermal Environment — Analytical Determination and Interpretation of Thermal Comfort Using Calculation of the PMV and PPD Indices and Local Thermal Comfort Criteria* (2005).

31. ANSI/ASHRAE, *Thermal Environmental Conditions for Human Occupancy* 7 (2017).

32. P. O. Fanger, *Thermal Comfort* (Danish Tech. Press, 1970).

33. R. J. de Dear and G. S. Brager, "Developing an Adaptive Model of Thermal Comfort and Preference," *ASHRAE Transactions* 104, no. Pt 1A (1998): 145–167.

34. ANSI/ASHRAE, *ASHRAE Handbook: Fundamentals* 30329, no. 404 (2009)

35. E. Asadi, M. G. Da Silva, C. H. Antunes, and L. Dias, "A Multi-Objective Optimization Model for Building Retrofit Strategies Using Trnsys Simulations, Genopt and MATLAB," *Building and Environment* 56 (2012): 370–378.

36. Y. Zhang, "Use jEPlus as an Efficient Building Design Optimisation Tool," CIBSE ASHRAE Technical Symposium, Imperial College, April 19, London, UK (2012) 18.

37. Department for Education, Energy Efficiency: Guidance for the School and Further Education College Estate, Gov.Uk (2022) 1–18, https://www.gov.uk/government/publications/energy-efficiency-guidance-for-the-school-and-fe-college-estate/energy-efficiency-guidance-for-the-school-and-further-education-college-estate.

38. ANSI/ASHRAE, *ANSI/ASHRAE Standard 62.1-2022, Ventilation and Acceptable Indoor Air Quality* (2022).

39. CIBSE. *Environmental Design, CIBSE guide A* (2021), https://doi.org/10.5040/9781472596178-bed-e035.

40. R. Daniels, *Building Bulletin 101 Guidelines on Ventilation, Thermal Comfort and Indoor Air Quality in Schools Version 1* (2018).

41. Z. Wang and G. P. Rangaiah, "Application and Analysis of Methods for Selecting an Optimal Solution From the Pareto-Optimal Front Obtained by Multiobjective Optimization," *Industrial & Engineering Chemistry Research* 56, no. 2 (2017): 560–574, https://doi.org/10.1021/acs.iecr.6b03453.

42. F. Ciardiello and A. Genovese, "A Comparison Between TOPSIS and SAW Methods," *Annals of Operations Research* 325, no. 2 (2023): 967–994, https://doi.org/10.1007/s10479-023-05339-w.

43. H. Taherdoost, "Analysis of Simple Additive Weighting Method (SAW) as a MultiAttribute Decision-Making Technique: A Step-by-Step Guide," *Journal of Management Science & Engineering Research* 6, no. 1 (2023): 21–24, https://doi.org/10.30564/jmser.v6i1.5400.

44. N. Meghanathan, "Assortativity Analysis of Real-World Network Graphs Based on Centrality Metrics," *Computer and Information Science* 9, no. 3 (2016): 7, https://doi.org/10.5539/cis.v9n3p7.

45. J. D. Evans, *Straightforward Statistics for the Behavioral Sciences*, 1st ed. (Brooks Cole Publishing Company, 1995).

46. S. Silva, A. Monteiro, M. A. Russo, et al., "Modelling Indoor Air Quality: Validation and Sensitivity," *Air Quality, Atmosphere & Health* 10, no. 5 (2017): 643–652, https://doi.org/10.1007/s11869-016-0458-4.

47. S. J. Emmerich and D. Hirnikel, "Validation of Multizone IAQ Modeling of Residential-Scale Buildings: A Review," *ASHRAE Transactions* 107, no. PART 2 (2001): 619–628.

48. A. Abbaspour, H. Seraj, A. Bahadori-Jahromi, and A. Janbey, "Performance of Ventilation, Filtration, and Upper-Room UVGI in Mitigating $PM_{2.5}$ and SARS-CoV-2 Levels," *Clean Technologies* 7, no. 3 (2025): 53, https://doi.org/10.3390/cleantechnol7030053.